Mechanics of Semifluidization of Single Size Particles in Solid-Liquid Systems

LIANG-TSENG FAN

Kansas State University, Manhattan, Kansas

CHIN-YUNG WEN

West Virginia University, Morgantown, West Virginia

Mechanical and dynamical characteristics of semifluidized beds of single-size particles in solid-liquid system were investigated. A semifluidized bed is a type of fluidized bed in which the bed expansion is partially restricted. The emphasis was placed on the study of packed bed formation and pressure drop increase when the semifluidized beds were formed by the compression of fluidized beds. The data showed good agreement with the theoretical and semiempirical equations based on a simple model of fluidized beds.

The results of this investigation would also contribute to the understanding of fluidized beds.

In a fluidized bed the suspended particles are in constant motion, but they occupy finite volume in the container just as a given quantity of water occupies a finite volume in a given vessel (*13*). As a rate of the upward flow of fluid through the suspension increases, the volume or height of the suspension increases provided free expansion of the suspension is permitted. The pressure loss of the fluid through the suspension of fluidized solid particles remains practically independent of the flow rate. But the pressure loss of a fluid flowing through the suspension of solid particles would be expected to increase when the free expansion of the bed is restricted.

Restriction of the expansion of the fluidized suspensions can be produced by placing at the top of the suspension a porous plate which passes the fluid but prevents the passage of the solid particles. A bed of restricted expansion thus obtained is called a *semifluidized bed* (*8, 9*). The semifluidized bed should be considered a special case of the general vertical fluidized systems (*12, 17, 20*). The advantages of the semifluidized bed over conventional fixed and fluidized beds are described in the previous papers (*8, 9*).

The purpose of this article is to report the results of investigation on mechanical and dynamic characteristics of semifluidization. The emphasis is placed on the study of formation of packed bed section and pressure drop in a semifluidized bed of single size particle systems.

A systematic investigation of the fluidized particles suspension under restricted expansion was reported previously (8, 9). The initial phase of the investigation was mainly concerned with convective mass transfer from the surface of the solid particles to the fluid. In the course of the mass transfer study it was found that upon the restriction of expansion of fluidized suspension the particles were separated into two distinctly visible phases. In one of the phases all the solid particles were rigidly packed in a fixed position, forming a fixed bed or packed bed just below the top porous plate. The rest of the particles remained fluidized in suspension below the packed phase.

THEORETICAL

Under the assumptions that the particles are uniformly distributed in a fluidized bed (*18*); the movement of a particle in the suspension is completely independent of other particles (*18*), and the suppression of the expansion of the suspensions and subsequent formation of the packed section does not change the average particle distance in the fluidized section (8); and the voidage of the packed section is constant and is that of the least dense static bed under resting conditions, the following equation for the height of the packed section can be obtained (*8*):

$$h_{pa} = (h_f - h)\,\frac{1-\epsilon_f}{\epsilon_f - \epsilon_{pa}} \qquad (1)$$

This equation is based on the material balance between the completely fluidized and suppressed states of the suspension.

Considerable success has been achieved in the study of the behavior of suspension in sedimentation and fluidization of spherical single size particles by assigning stable geometrical arrangements to the particles in suspension (*10, 14, 18*). McNoun (*14*) considered that each particle in suspension is situated in the center of a normal hexagon of fluid. The vertical distance between the layers of the particles was considered as equal to the distance between the particles in a horizontal direction. Hawksley (*10*) also considered the particles as being situated at the center of a normal hexagon of fluid but regarded the layers of the particles being arranged in adjacent horizontal layers so as to offer the minimum resistance to the motion of a fluid.

Following the first assumption let L_1, L_2, and L_3 be the three characteristic dimensions of the average space occupied by a single particle in a fluidized bed. Then the volume of this space may be represented as $\alpha_1 L_1 L_2 L_3$. Similarly the volume of the particle itself can be represented as $\beta b_1 b_2 b_3$. Then the porosity of the fluidized bed is

$$\epsilon_f = 1 - \frac{\beta b_1 b_2 b_3}{\alpha_1 L_1 L_2 L_3} \qquad (2)$$

The average number of particles situated in any cross section of the fluidized bed is

$$n_f = \frac{A}{\gamma_1 L_1 L_2} \qquad (3)$$

By a similar treatment

$$\epsilon_{pa} = 1 - \frac{\beta b_1 b_2 b_3}{\alpha_2 b_1 b_2 b_3} = 1 - \frac{\beta}{\alpha_2} \qquad (4)$$

and

$$n_{pa} = \frac{A}{\gamma_2 b_1 b_2} \qquad (5)$$

From Equations (2) and (4)

$$\frac{1-\epsilon_{pa}}{1-\epsilon_f} = \frac{\alpha_1 L_1 L_2 L_3}{\alpha_2 b_1 b_2 b_3} \qquad (6)$$

The number of particle layers in the fluidized bed required to form one layer of the packed section will be

$$\frac{n_{pa}}{n_f} = \frac{\gamma_1 L_1 L_2}{\gamma_2 b_1 b_2}$$

Consequently the height to be suppressed to form N layer of the packed bed is

$$h_f - h = N\left[\left(\frac{\alpha_1 L_1 L_2 L_3}{\gamma_1 L_1 L_2}\right)\left(\frac{\gamma_1 L_1 L_2}{\gamma_2 b_1 b_2}\right) - \left(\frac{\alpha_2 b_1 b_2 b_3}{\gamma_2 b_1 b_2}\right)\right] \qquad (7)$$

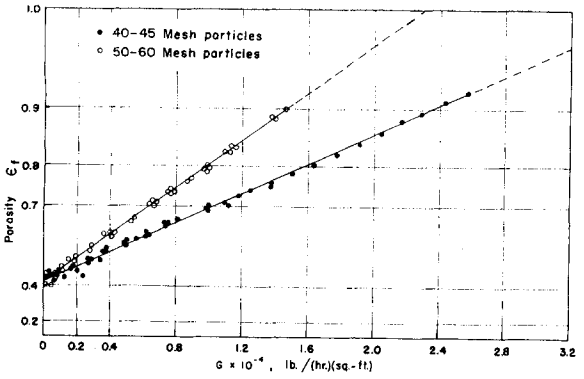

Fig. 1. Porosity of fully fluidized beds of 40- to 45-mesh particles and 50- to 60-mesh particles.

Since

$$h_{pa} = N\frac{\alpha_2 b_1 b_2 b_3}{\gamma_2 b_1 b_2}$$

$$h_f - h = h_{pa}\left[\left(\frac{\alpha_1 L_1 L_2 L_3}{\alpha_2 b_1 b_2 b_3}\right) - 1\right] \quad (8)$$

Substitution of Equation (6) in Equation (8) yields Equation (1). In this derivation no particular shape is assigned to the particles except that statistically speaking they can be represented by the same characteristic dimensions. Experimental data (*8, 9*) substantiated the validity of Equation (1) for the benzoic acid particles whose geometry is far from spherical and whose dumped porosity is considerably greater than that predicted for the orthorhombic arrangement.

The increases of the pressure drop across the fluidized suspension as its expansion is restricted can be considered to correspond to the increases of pressure as the gas is compressed.

There are a number of semiempirical or theoretical equations which have been proposed to predict the pressure loss in a fluid across a bed of solid particles (*4, 5, 6, 7, 13, 15*). Because of the formation of the packed section when the fluidized suspension was suppressed, the total pressure drop should be the algebraic sum of the pressure drops across the fluidized section and the packed section, since these two sections are aligned in series in the direction of fluid flow. Therefore

$$\Delta P_t = \left(\frac{\Delta P}{L}\right)_f (h - h_{pa}) + \left(\frac{\Delta P}{L}\right)_{pa} h_{pa} \quad (9)$$

Since the pressure drop through a suspension of fluidized solid particles is equal to their effective weight

$$\left(\frac{\Delta P}{L}\right)_f (h - h_{pa}) = \frac{(1-X)W}{A}\frac{(\rho_s - \rho_f)}{\rho_s} \quad (10)$$

X can be calculated by means of Equation (1) as follows:

$$X = \frac{A\rho_s(1-\epsilon_{pa})h_{pa}}{W} = \frac{(1-\epsilon_{pa})(h_f - h)}{h_f(\epsilon_f - \epsilon_{pa})} \quad (11)$$

When Ergun's equation is employed (*4, 5, 6, 7*)

$$\left(\frac{\Delta P}{L}\right)_{pa} h_{pa} = \left[150\frac{(1-\epsilon_{pa})^2}{\epsilon_{pa}^3}\frac{\mu u}{d_p^2} + 1.75\frac{(1-\epsilon_{pa})}{\epsilon_{pa}^3}\frac{Gu}{d_p}\right]\left[(h_f - h)\frac{(1-\epsilon_f)}{(\epsilon_f - \epsilon_{pa})}\right] \quad (12)$$

Consequently the pressure drop through a semifluidized bed may be estimated as

$$\Delta P_t = \left\{\left[h_f - \frac{(1-\epsilon_{pa})(h_f - h)}{\epsilon_f - \epsilon_{pa}}\right](1-\epsilon_f)(\rho_s - \rho_f)\right\} + \left[150\frac{(1-\epsilon_{pa})^2}{\epsilon_{pa}^3}\frac{\mu u}{d_p^2} + 1.75\frac{(1-\epsilon_{pa})}{\epsilon_{pa}^3}\frac{Gu}{d_p}\right]\left[(h_f - h)\frac{(1-\epsilon_f)}{\epsilon_f - \epsilon_{pa}}\right] \quad (13)$$

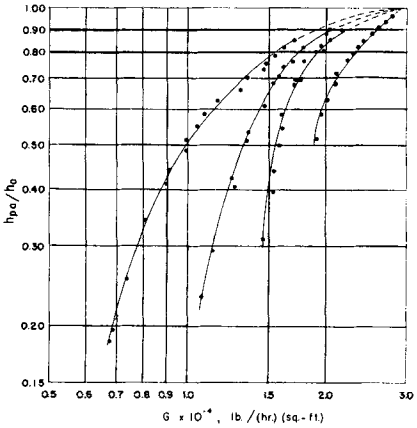

Fig. 2. h_{pa}/h_o vs. water flow rate. Evaluation of maximum semifluidization velocity for 50 to 60 mesh (A series).

EXPERIMENTAL

Two sizes of spherical glass beads and water were used. The properties of the glass beads used were as follows: ϵ_o = 0.424, ρ_s = 154.1 lb./cu.ft., d_p = 0.0098 to 0.0119 in. for 50- to 60-mesh particles and ϵ_o = 0.426, ρ_s = 154.1 lb./cu.ft., d_p =0.0138 to 0.0164 in. for 40- to 45-mesh particles.

The restriction of the expansion of the fluidized bed was achieved by placing a porous plate at a predetermined height shorter than that of the height of the fully fluidized bed.

As shown in the previous section the analysis of the semifluidization data requires an accurate knowledge of the fully fluidized bed operated under the same flow conditions. Such experiments were conducted in order to measure the bed expansion characteristics and the porosity of the fully fluidized beds. These results essential to the analysis of semifluidization data are presented also.

After a weighed quantity of the solid particles was charged into the column, the bed was fluidized and resettled in order to obtain reproducible readings of the initial height of the static bed. Then the velocity of the water was increased very slowly up to a present velocity at which the desired compression of the fluidized bed was produced. The gradual increase of the velocity of water minimized the compression of the packed section already formed. Upon reaching the steady state operation the height of packed section, the over-all pressure drop, and operating conditions were recorded. The data presented were the average of several readings taken for each experimental run.

RESULTS

The fluidization data obtained are listed in Table 1, and the semifluidization data are summarized in Table 2*. The same series numbers are used for the corresponding fluidization and semifluidization experiments and are distinguished by the low case *f* and *s* at the end of the experimental series number respectively. The porosities of fully fluidized beds are plotted in Figure 1 to be used for the purpose of interpolation and extrapolation required in the analysis of semifluidization data. Figure 1 shows that a good linear relationship exists between ln $(1.1 - \epsilon_f)$ and flow scale G. Inversed ln $(1.1 - \epsilon_f)$ scale is used in Figure 1.

While the minimum flow rate of fluid required to produce semifluidiza-

* Tabular material is deposited as document 6890 with the American Documentation Institute, Photoduplication Service, Library of Congress, Washington, D.C., and may be obtained for $2.50 for photoprints or $1.75 for 35-mm. microfilm.

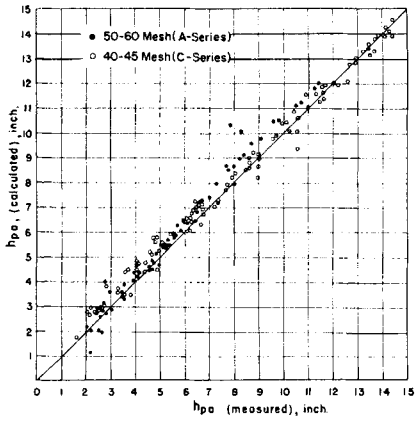

Fig. 3. Comparison of measured heights of packed section with theoretical values for 50- to 60-mesh particles (A series) and 40- to 45-mesh particles (C series).

tion depends on the static bed height relative to the over-all bed height, the maximum flow rate at which semifluidization is possible corresponds to the terminal (free fall) velocity of the particles for the column geometry used in this work. Above this velocity all the particles will be in the packed section. Therefore maximum semifluidization may be obtained by three methods: (a) by linear extrapolation of ϵ_f vs. G curves, as shown in Figure 1, to $\epsilon_f = 1$; (b) by extrapolation of h_{pa}/h_o vs. G to $h_{pa}/h_o = 1.0$ as shown in Figure 2; (c) by calculation of free fall terminal velocity. Method (a) is based on the fact that above the maximum semifluidization velocity (which is also the maximum fluidization velocity) all the particles, if the bed expansion is not restricted, would have been carried out of the column and consequently the porosity of the bed would approach unity. Method (b) is based on the fact that all the particles are shifted to the packed section from the fluidized section at the maximum semifluidization point. Therefore the height of the packed section at this point becomes equal to that of static bed height provided that the third assumption made in the previous section is valid.

Method (c) is based on a proposition that at the maximum semifluidization point the settling velocity of individual particles becomes equal to the upward flowing fluid velocity. Under the condition of the present investigation the intermediate law for the gravity settling was valid. Intermediate law is expressed as

$$G_t = 0.152 \frac{d_p^{1.14}\, g_c^{0.714}\, (\rho_s - \rho_f)^{0.714}}{\mu^{0.428}\, \rho_f^{0.286}} \qquad (14)$$

The maximum semifluidization velocities determined by these three methods are listed in Table 3. The causes for the discrepancies are discussed in the following section.

In Figure 3 the observed heights of the packed section listed in Table 2 are plotted for comparison with the values calculated in accordance with Equation (1). The over-all pressure drop of both fully fluidized and semifluidized beds are plotted in Figure 4.

DISCUSSION AND CONCLUSION

It has been recognized (*1, 13*) that some degree of fluctuation of the solid density cannot be avoided in any fully fluidized bed. It was observed that the concentration of solid particles was lower at the upper section of the fully fluidized beds; as the water flow rate was increased, the section of low solid concentration expanded in proportion. Such stratification of solid particles naturally affects the porosity of the bed. The over-all porosity ϵ_f is in general greater than that based on the main body of the fluidized bed under a given flow rate. Thus the extrapolation to $\epsilon_f = 1$ from the plot of ϵ_f vs. G gives the lower value of G_t than can be obtained based on the uniform bed density distribution.

The maximum semifluidization velocities determined by method (b) G_t'' (those determined by extrapolation of h_{pa}/h_o vs. G curves to the $h_{pa}/h_o = 1$) were always greater than the values determined by method (a), probably owing to the following two reasons.

Even though very close cut particles were used in the experiments, there was a definite size distribution for every sample. The maximum semifluidization velocity (or free fall velocity) of the largest particles should be greater than that of the average size particle. Until all the particles including the largest particles are transferred from the fluidized section to the packed section the values of h_{pa}/h_o would not reach 1. This means that the maximum semifluidization velocity determined by this method is greater than the values obtained for the completely uniform particles of the average size.

One of the basic assumptions involved in method (b) is that the porosity of the packed section formed remained equal to that of the least dense static bed prior to fluidization. Although this assumption was found to be almost true, as will be shown later, the packed section tended to become slightly compressed as the velocity of the water was increased. This, in turn, made the value of maximum semifluidization velocity obtained by method (b) greater than it should be when the packed section remained at the least dense condition.

TABLE 3. MAXIMUM SEMIFLUIDIZATION VELOCITY

Experimental series (particles)	Maximum semifluidization velocity Method (a)* G_t', lb./hr.-sq. ft.	Method (b)† G_t'', lb./hr.-sq. ft.	Method (c)** G_t, lb./hr.-sq. ft.
A (50-60 mesh)	23,000	28,000	21,100
C (40-45 mesh)	36,600	40,000	33,500

* Method (a): ϵ_f vs. G plot.
† Method (b): h_{pa}/h_o vs. G plot.
** Method (c): calculation.

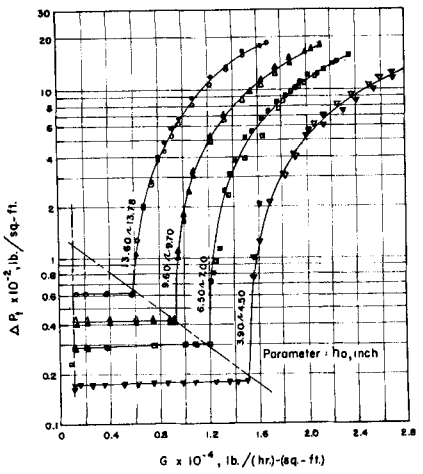

Fig. 4. Over-all pressure drop through fully and semifluidized beds of 50- to 60-mesh particles (A series).

The difference of the maximum semifluidization velocities estimated by method (c) from the values determined by either of the previous methods cannot be explained merely as due to the experimental error. The intermediate equation for gravity settling is derived for a single particle. There must be a definite influence of the existence of other particles, as well as the effect of column wall and supporters.

From the standpoint of the semifluidization only the values obtained by method (b) can be strictly defined as maximum semifluidization velocity because they were actually determined under the operating conditions of semifluidization. It can be seen in Table 2 that some experimental runs were made above G_t' [method (a)] but always below G_t'' [method (b)].

Minimum semifluidization velocity

While the maximum semifluidization velocity depends on characteristics of the particles and the fluidizing fluid, the onset velocity of semifluidization (or minimum semifluidization velocity) depends, in addition, on the quantity of the particles in relation to the column size, that is h_o/h ratio. When the value of h_o/h is unity, the onset velocities of semifluidization could be obtained from the pressure drop vs. flow

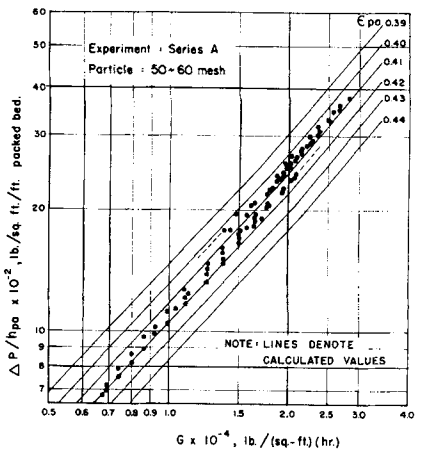

Fig. 5. Comparison of experimental pressure drop data with calculated values with various porosity.

rate plots. Theoretically in this case the semifluidization sets in at the moment the fluidization starts. However when the value of h_o/h approaches zero, the semifluidization cannot be produced until the fluid velocity reaches the terminal velocity of the particles.

Height of Packed Section

The close agreement between the theoretical values and experimental data shown in Figure 3 substantiates the validity of the theoretical equation, Equation (1), for height of packed section for the single size particles. This leads to the conclusion that the various assumptions made with respect to the characteristics of fluidized beds in deriving the equation are valid. It has already been pointed out that Equation (1) was found to be valid for nonspherical particles (*8, 9*).

Pressure Drop

One of the uncertainties in the use of Equation (13) to estimate the over-all pressure drops is the knowledge of porosity of the packed section. It is known that any available equations for estimating the pressure drop of the packed beds are quite sensitive to the variation of the bed porosity. Furthermore there are no direct ways of simultaneously measuring the porosity in fluidized and in packed sections for the semifluidized beds. As mentioned previously the validity of Equation (1) indicates that the use of the porosity of the least dense static bed for the packed section is satisfactory. This has also been proved as follows. The data shown in Figure 4 are replotted on a slightly different basis in Figure 5 and are compared with the calculated lines by assigning various values to the porosity of the packed section. From Figure 5 the best calculated line fitting the experimental data is seen to correspond to the mean porosity of the least dense static bed. But a slight effect of compression of the packed section with an increase of the water flow rate is also observed.

Curves A, B, C, and D in Figure 6 all represent the pressure drops of the various modes of a particle bed when they are operated under the conditions of experiment series A-I-2. Curve A represents the case when no expansion of the static bed is allowed above the onset velocity of fluidization. Curve B which agrees with the experimental data closely represents Equation (13), that is the pressure drop equation of semifluidized bed based on Ergun's equation. It is known that Ergun's equation is not only valid to the densely packed beds but also to the very loosely packed beds (*4, 5, 6, 7*). Calculation of Curve C is based on the assumption that the particles inside the bed are uniformly distributed between the bottom supporting screen and the top compressing porous plate instead of forming packed and fluidized sections as actually observed. In other words this curve represents a hypothetical particle-fluid bed in which the distances between the particles reduce uniformly upon the compression of the bed.

Curve D represents the pressure drop of the same bed when it is fully fluidized.

Analogy between mass and momentum transfers

In the previous mass transfer study (*9*) it has been indicated that the over-all mass transfer coefficients between the solid particle surfaces and fluid can be expressed as weighted average of the mass transfer coefficients in the packed section and in the fluidized section. The analogical situation is observed in Equation (13) for the over-all pressure drop through the semifluidized bed. The average pressure drop per unit depth of the bed may be considered a weighted value between the two sections. It is further indicated in the previous work that the over-all mass transfer coefficients can be approximated by use of the various generalized correlations for mass transfer coefficients which cover both fluidized and packed beds (*8, 9*). However this is not the case for the pressure drop as shown in Figure 6. The over-all pressure drops estimated by use of the over-all porosity of the bed are well below those of the experimental data. This breakdown of the analogy, especially at the high flow rate, is due to the fact that form drag in addition to the skin friction become appreciable at high rate of fluid flow. It is known that the surface to fluid mass transfer finds the analogy only in the skin drag on the particles.

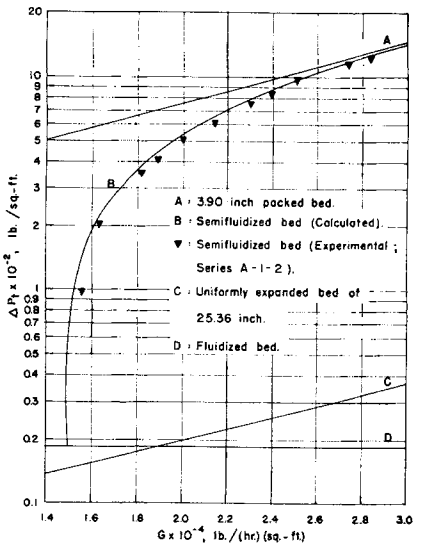

Fig. 6. Pressure drops for various modes of particle-fluid beds.

Dimensionless correlation of packed height

Dimensional analysis by use of the momentum and continuity equation for particulate fluidization leads to the expression (*2, 3*)

$$f\left(\frac{\epsilon_f - \epsilon_o}{1 - \epsilon_o}, \frac{u - u_{mf}}{u_t - u_{mf}}\right) = 0 \quad (15)$$

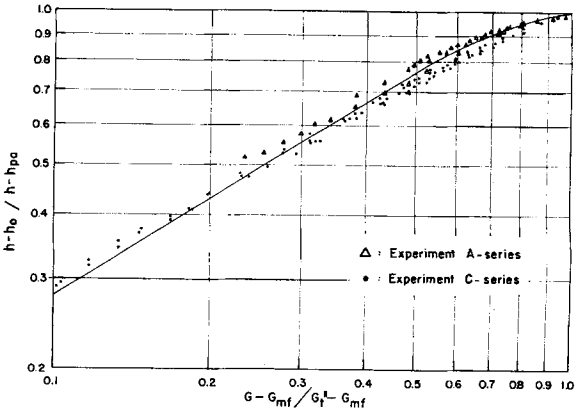

Fig. 7. Dimensionless correlation for semifluidized bed formation with maximum semifluidization velocity determined by method (b).

Since $h_f = h_o R$ and $R = \frac{1-\epsilon_o}{1-\epsilon_f}$, from Equation (1)

$$h_{pa} = \left(\frac{1-\epsilon_o}{1-\epsilon_f} h_o - h\right) \frac{1-\epsilon_f}{\epsilon_f - \epsilon_{pa}}$$

$$= \frac{1-\epsilon_o}{\epsilon_f - \epsilon_{pa}} h_o - \frac{1-\epsilon_{pa}}{\epsilon_f - \epsilon_{pa}} h + h$$

Since ϵ_{pa} is practically equal to ϵ_o

$$h_{pa} = \frac{1-\epsilon_o}{\epsilon_f - \epsilon_o} h_o - \frac{1-\epsilon_o}{\epsilon_f - \epsilon_o} h + h$$

or

$$\frac{h-h_o}{h-h_{pa}}, = \frac{\epsilon_f - \epsilon_o}{1-\epsilon_o} \quad (16)$$

Substituting this relationship into Equation (15) one gets

$$f\left(\frac{h-h_o}{h-h_{pa}}, \frac{G-G_{mf}}{G_t - G_{mf}}\right) = 0 \quad (17)$$

This indicates that a unique relationship exists between the two dimensionless factors in the equation regardless of the characteristics of the system.

The first factor $h-h_o/h-h_{pa}$ may be considered to be associated with the over-all expansion allowed for semifluidized bed and the fraction of packed height (or the dimensionless packed height) because

$$\frac{h-h_o}{h-h_{pa}} = \frac{1-\frac{1}{h/h_o}}{1-\frac{h_{pa}}{h}}$$

The second factor $G-G_{mf}/G_t-G_{mf}$ may be considered a normalized semifluidization velocity which numerically ranges from 0 to 1.

The dimensionless relationship based on Equation (17) is illustrated in Figure 7. The curve in the figure represents the theoretical curve obtained by calculating each term in dimensionless relationship by means of Equation (1) and the knowledge of the fully fluidized beds (the bed expansion as a function of the flow rate). The onset velocities of fluidization required in evaluating the second dimensionless factor were calculated by the following equation derived by Leva et al. (*13*) and recently theoretically justified by Shannon (*19*):

$$G_{mf} = 688\, d_p^{1.82} \frac{[\rho_f (\rho_s - \rho_f)]^{0.94}}{\mu^{0.88}} \quad (18)$$

The observation of Figure 7 indicates that the experimental data and the theoretical curve show good agreement.

ACKNOWLEDGMENT

This work was partly financed by National Science Foundation Grant G-14300.

The authors also wish to acknowledge the assistance given by Messrs. T. C. Chen and C. J. Lee of Kansas State University.

NOTATION

A = cross section of column, sq. ft.

b_1, b_2, b_3 = characteristic dimensions of particle, ft.

d_p = particles diameter, ft. or in.

f, f' = function

g_c = conversion factor, lb.-mass/lb.-force-ft./hr.^{2}

g = gravitational acceleration, ft./hr.^{2}

G = flow rate of water, lb./(sq. ft.)(hr.)

G_{mf} = onset velocity of fluidization, lb./(sq. ft.)(hr.)

G_t = free fall terminal velocity (maximum semifluidization velocity) calculated, lb./(sq. ft.)(hr.)

G_t' = maximum semifluidization velocity from ϵ_f vs. G plot, lb./(sq. ft.)(hr.)

G_t'' = maximum semifluidization velocity from h_{pa}/h_o vs. G plot, lb./(sq. ft.)(hr.)

h = over-all height of column (or semifluidized bed), ft. or in.

h_f = height of fully fluidized bed, ft. or in.

h_o = height of initial static bed at least dense condition, ft. or in.

h_{pa} = height of packed section in semifluidized bed, ft. or in.

L_1, L_2, L_3 = characteristic dimensions of space occupied by one particle in fluidized bed, ft.

N = number of layers of particles in packed section

n_f = number of particles in cross section of column in fluidized sections

n_{pa} = number of particles in cross section of column in packed section

ΔP_t = over-all pressure drop, lb./sq. ft.

ΔP_f = pressure drop through fluidized section, lb./sq. ft.

ΔP_{pa} = pressure drop through packed section, lb./sq. ft.

R = bed expansion ratio

u = velocity of fluid, length/time

u_t = terminal velocity of particle, length/time

W = total weight of particles in column, lb.

X = weight fraction of particles in packed section

Greek Letters

α_1 = volumetric coefficient for space occupied by single particle, in fluidized section

α_2 = volumetric coefficient for space occupied by single particle, in packed section

β = volumetric coefficient for volume of single particle

γ_1 = coefficient of cross-sectional area for space occupied by single particle in fluidized section

γ_2 = coefficient of cross-sectional area for space occupied by single particle in packed section

Δ = finite change of variable

ϵ_f = porosity of fluidized section or porosity of fully fluidized bed

ϵ_o = porosity of least dense static bed under resting condition

ϵ_{pa} = porosity of packed section

μ = viscosity of fluid, lb./(ft.)(hr.) or centipoise

ρ_f = density of fluid, lb./cu. ft.

ρ_s = density of solid particle, lb./cu. ft.

LITERATURE CITED

1. Baumgarten, P. K., Ph.D. thesis, Univ. of Delaware, Newark, Delaware (1956).
2. Beranek, I. J., *Brit. Chem. Eng.*, **3**, 358-363 (1958).
3. ———, and T. Klumpar, *Collection Czechoslov, Chem. Commun.*, **23**, 1-29 (1958).
4. Ergun, Sabri, *Chem. Eng. Progr.*, **48**, 89 (1952).
5. ———, *Anal. Chem.*, **23**, 151 (1951).
6. *Ibid.*, **24**, 388 (1952).
7. Ergun, Sabri, and J. Owen, *ibid.*, **25**, 1222 (1953).
8. Fan, L. T., Y. C. Yang, and C. Y. Wen, *A.I.Ch.E. Journal*, **5**, 407, (1959).
9. *Ibid.*, **6** 482 (1960).
10. Hawksley, P. G., "Symposium: Some Aspects of Fluid Flow," Edward Arnold and Company, London, England (1950).
11. Katz, H. M., *Argonne Natl. Lab. Rept. No. ANL-5725* (1957).
12. Lapidus, Leon, and J. C. Elgin, *A.I.Ch.E. Journal*, **3**, 63 (1957).
13. Leva, Max, T. Shirai, and C. Y. Wen, *Genie Chim.*, **75**, 33 (1956).
14. McNoun, J. S., et al., *Proc. Int. Congress Appl. Mech.*, **7**, No. 11, p. 17.
15. Morse, R. D., *Ind. Eng. Chem.*, **41**, 1117-1124 (1949).
16. Omae, T., and J. Furukawa, *J. Chem. Soc. Japan*, Ind. Chem. Sect., **56**, 727-31 (1953).
17. Price, B. G., Leon Lapidus, and J. C. Elgin, *A.I.Ch.E. Journal*, **5**, 93 (1959).
18. Richardson, J. F., and W. N. Zaki, *Chem. Eng. Sci.*, **3**, 65 (1954).
19. Shannon, P. T., Ph.D. thesis, Ill. Inst. Technol., Chicago, Illinois (1959).
20. Struve, D. L., Leon Lapidus, and J. C. Elgin, *Can. J. Chem. Eng.*, **36**, 141 1958).

Manuscript received September 20, 1960; revision received April 17, 1961; paper accepted April 19, 1961.